Nano Today (2009) xxx, xxx—xxx

available at www.sciencedirect.com

ScienceDirect

journal homepage: www.elsevier.com/locate/nanotoday

RAPID COMMUNICATION

Enhanced pyroelectric crystal D—D nuclear fusion using tungsten nanorods

Donald J. Gillich[a], Ranganath Teki[b], Travis Z. Fullem[a], Andrew Kovanen[a], Ezekiel Blain[a], Douglas B. Chrisey[d], Toh-Ming Lu[c], Yaron Danon[a,*]

[a] *Department of Mechanical, Aerospace, and Nuclear Engineering, Rensselaer Polytechnic Institute, Troy, NY 12180, United States*
[b] *Department of Chemical Engineering, Rensselaer Polytechnic Institute, Troy, NY 12180, United States*
[c] *Department of Physics, Applied Physics, and Astronomy, and Center for Integrated Electronics, Rensselaer Polytechnic Institute, Troy, NY 12180, United States*
[d] *Department of Materials Science and Engineering, Rensselaer Polytechnic Institute, Troy, NY 12180, United States*

Received 16 January 2009; received in revised form 27 February 2009; accepted 19 April 2009

KEYWORDS
Pyroelectric crystal;
Neutrons;
Tungsten nanorods;
Oblique angle deposition

Summary Thin films of vertically aligned tungsten nanorods were used to enhance field ionization in pyroelectric crystal D—D fusion experiments resulting in increased neutron production. The tungsten nanorods were deposited on a single $LiTaO_3$ crystal using sputter deposition at glancing angles. The combination of a single tungsten tip with a thin film of nanorods on the face of the crystal yielded about four times the number of neutrons than did either a single tip or nanorods alone.

Introduction

Pyroelectric crystals have been used to achieve D—D fusion through the ionization of deuterium gas and acceleration of these ions into a deuterated target. Pyroelectric-generated fusion (pyrofusion) was first achieved in 2005 by the University of California at Los Angeles (UCLA) [1] and the phenomenon was confirmed in 2006 by Rensselaer Polytechnic Institute (RPI) [2]. In December 2007, Lawrence Livermore National Lab (LLNL) reported that a pyroelectric crystal driven neutron source is operational and has achieved a record yield of 1.9×10^5 neutrons per thermal cycle using a single crystal [3].

Previously, a single 70 nm radius tungsten (W) tip was used to locally enhance the electric field generated by pyroelectric crystals which increases deuterium gas ionization and thereby the neutron yield [1—3]. Experiments have shown that these tips erode over time which reduces the initial field ionization enhancement [3,4]. Ref. [4] shows pictures of tip erosion from a 70 nm to ~2 μm radius after 10 experiments. The current density during each of these experiments is estimated to be ~16 A/cm^2. The results reported here include the use of nanorods on the crystal surface in conjunction with a single tip, thereby increasing the number of ''tips'' available to enhance the ionization process.

The primary goal of this research at RPI was to improve the efficiency of ionization which will in turn increase

* Corresponding author. Tel.: +1 518 276 4008; fax: +1 518 276 4832.
E-mail address: danony@rpi.edu (Y. Danon).

1748-0132/$ — see front matter © 2009 Elsevier Ltd. All rights reserved.
doi:10.1016/j.nantod.2009.04.004

the yield of neutrons generated by deuterium–deuterium (D–D) fusion closer to the theoretical limit. Using a system of two 30 mm diameter $LiTaO_3$ crystals with an average ion acceleration potential of 180 kV, pyroelectric crystal neutron generators using D–D fusion are expected to yield about 1×10^7 neutrons per emission cycle, which is generally around 100 s [5]. The same generator using a deuterium–tritium (D–T) reaction would increase the yield by about 300 giving a total theoretical neutron yield of 3×10^7 neutrons per second.

A pyroelectric crystal is a ferroelectric material that exhibits spontaneous polarization which changes when the crystal is heated or cooled. (These crystals are usually cut such that the maximum dipole moment from each unit cell is perpendicular to the flat surfaces, the −z and +z faces.) Spontaneous polarization, P_s, is defined as the dipole moment per unit volume of the material and is non-zero for pyroelectric materials [6]. During equilibrium conditions (when the temperature is constant), an equivalent surface charge will assemble at the faces of the crystal to screen the charge due to P_s. A pyroelectric crystal has a Curie temperature above which the crystal loses its pyroelectric properties. The Curie temperature for $LiTaO_3$ is reported to be 685 °C [7].

When the crystal is heated, P_s decreases and equivalent surface charge from the surrounding environment compensates for this change at the crystal face. Consider the +z face in a system being heated. As P_s decreases the crystal surface becomes less positive and positive ions are attracted toward the crystal face to compensate this change while electrons are accelerated away from the crystal face. During cooling, the process is reversed: P_s increases making the +z face more positive and electrons are accelerated toward the crystal face while positive ions are accelerated away from it. The −z face exhibits the same behavior with opposite signs. See Fig. 1a for a graphical depiction of the change in charge at the crystal face during a thermal cycle. The change in charge distribution and the accompanying change in the electric field are used to achieve D–D pyrofusion. RPI uses a two-crystal system in which the +z face of one crystal is facing the −z face of the other crystal which doubles the acceleration potential [2].

During cooling, the electric field generated between the pyroelectric crystals is high enough to ionize D_2 gas. The ratio of D_2^+ to D^+ ionization is not clear. For the results reported by Tang et al. [3] at LLNL, neutron yield calculations indicated that the ion beam was predominantly D^+ and not D_2^+. However, previous attempts [8] to measure deuterium ion type for the RPI two crystal system showed no evidence of D^+. For a fixed acceleration potential, D^+ ions have a higher cross-section for D–D fusion than does D_2^+ because each deuterium atom in a D_2^+ ion will have half the kinetic energy of a D^+ ion accelerated to the same energy. During cooling, positive ions are accelerated away from a +z face while a −z face attracts the ions into a deuterated polyethylene (CD_2) target (see Fig. 1).

The change in spontaneous polarization, ΔP_s, causes a change in the amount of surface charge on each face of the crystal. The change in spontaneous polarization can be calculated by multiplying the change in temperature with

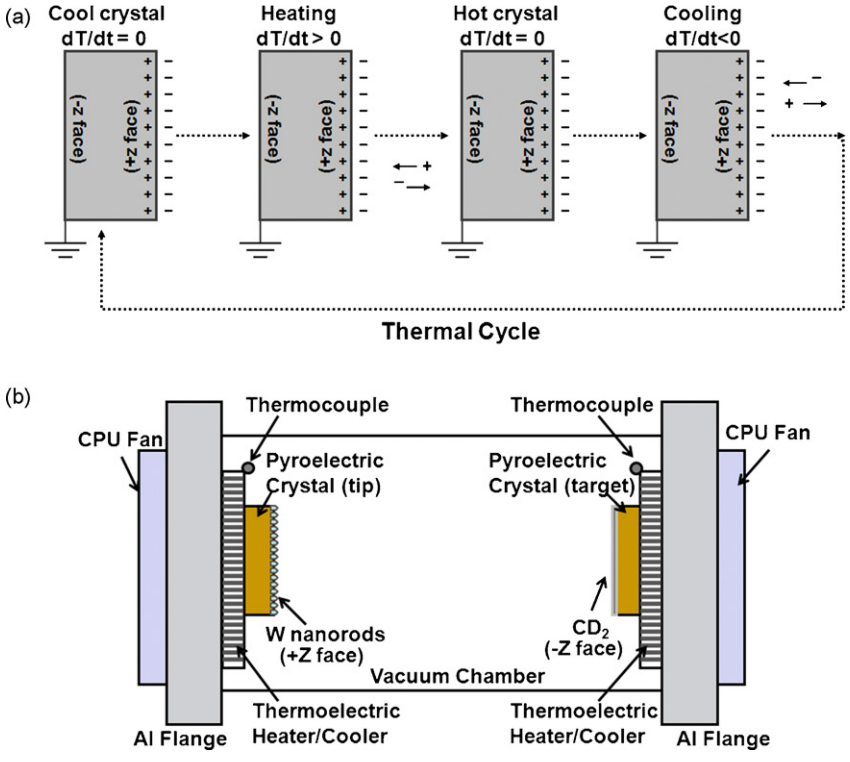

Figure 1 (a) Schematic diagram of the change in charge formation on the face of a pyroelectric crystal charge during heating and cooling. (b) Diagram of RPI's two-crystal system. The crystals are approximately 7 cm apart from each other. The distance from the target crystal to the face of the proton-recoil neutron detector is ~6.55 cm. A 70-nm radius tungsten tip was added to the center of the crystal coated with nanorods for some of the experiments.

Please cite this article in press as: D.J. Gillich, et al., Nano Today (2009), doi:10.1016/j.nantod.2009.04.004

the pyroelectric coefficient, γ, such that

$$\Delta P_s = \gamma \Delta T \tag{1}$$

where γ is usually in uC m^{-2} K^{-1} and ΔT is in K. The value [5] for γ is approximately 190 uC m^{-2} K^{-1} for the $LiTaO_3$ crystals at the operating temperature used for research at RPI and ΔT is about 100 K. In a vacuum environment in which screening charge is not readily available, Eq. (1) gives the amount of charge on the crystal face per square centimeter. To get the total charge on the surface of the crystal this value is multiplied by the crystal surface area, A; for a 30 mm diameter crystal the total charge is 13.4×10^{-6} C.

Using the charge on the crystal face, the accelerating potential and the magnitude of the electric field between the crystal and the target can be calculated. To calculate the potential, V, the capacitance of the system must be determined to use the equation

$$V = \frac{Q}{C} \tag{2}$$

where $Q = \Delta P_s A$ and C is the capacitance of the system. Typically, a single crystal–target system is modeled as two parallel plate capacitors added in parallel with one capacitor being the crystal itself and the other being the gap between the crystal and the target. The equation for potential becomes

$$V = \frac{\gamma \Delta T A}{\varepsilon_0 \varepsilon_{crystal}(A/d_{crystal}) + \varepsilon_0(A/d_{gap})} = \frac{\gamma \Delta T}{\varepsilon_0((\varepsilon_{crystal}/d_{crystal} + (1/d_{gap}))} \tag{3}$$

where A is the surface area, ε_0 and $\varepsilon_{crystal}$ are the permittivity of free space and the relative dielectric permittivity of the crystal, respectively (for $LiTaO_3$, $\varepsilon_{crystal} \approx 46$) and $d_{crystal}$ and d_{gap} are the crystal thickness and gap thickness, respectively [5].

The electric field generated in the gap between the crystal and the target can be calculated using

$$E = \frac{V}{d_{gap}} \approx \frac{\gamma \Delta T d_{crystal}}{\varepsilon_0 \varepsilon_{crystal} d_{gap}} \tag{4}$$

where V is the potential calculated in Eq. (3). The calculated potential and electric field from above can be used to predict the accelerating conditions affecting deuterium ions during pyroelectric fusion experiments. Using RPI's two-crystal system, the maximum accelerating potential measured is approximately 240 kV.

The tungsten tip is used to enhance the electric field locally which will improve ionization. Eq. (5) is used to calculate the field-enhancement factor near a tip given a ''hemisphere on a post'' model [9].

$$\alpha = \left(2 + \frac{L}{\rho}\right)\left(1 - \frac{L}{d}\right) \tag{5}$$

where L is the tip length ($\sim$1 cm), ρ is the radius of the tip (70 nm), and d is distance between the anode and cathode ($\sim$7 cm), which gives a field-enhancement factor, α, of 1.2×10^5. In the experiments reported here, the crystal with the tip was the anode and the crystal with the target was the cathode during cooling.

The two-crystal system used at RPI includes a +z face with a tip across from a −z face with a deuterated polyethylene target. Two 1-cm thick, 3 cm diameter $LiTaO_3$ crystals were used in these experiments. The crystals were approximately 7 cm apart from each other in the vacuum chamber. Fig. 1b depicts a diagram of the two-crystal system. For single tip experiments, a $\sim$26 mm diameter, $\sim$0.8 mm thick copper disk with a standard DIP (dual-inline package) socket soldered in the middle was mounted to the center of the +z face of a crystal using conductive epoxy (GC electronics part number 19-2092). A 70 nm radius tungsten tip was placed in the DIP socket.

A second type of experiment included W nanorods that were deposited directly onto the $LiTaO_3$ surface of the +z face to act as field-enhancing tips. Theoretically, one would expect an increase in ionization (and therefore neutron yield) with a crystal covered with nanorods due to an increased number of electric field-enhancing tips. However, to calculate this increase would be problematic because it is uncertain how many dominant nanorod tips are functioning on the crystal surface. Also, once one dominant tip (or a group of tips) erodes over the course of emission, other tips likely take their place.

A third set of experiments combined the two approaches to enhance field ionization: the crystal surface was coated with W nanorods and a 0.5 cm^2 copper square with a DIP socket and 70 nm radius tip was glued onto the center of the crystal surface with conductive epoxy. The 70 nm radius tip apex was approximately 1 cm above the crystal surface. The copper square was glued directly onto the W nanorod-coated surface such that the nanorods under the copper square did not contribute to ionization near the crystal surface. The crystals were attached onto thermoelectric heater/coolers (TECs) using conductive epoxy. Using the same epoxy, the TECs were attached to aluminum vacuum flanges which had CPU cooling fans attached to them outside the vacuum chamber to facilitate heat transfer.

The nanostructured crystal surface was formed using oblique angle deposition with substrate rotation. Oblique angle deposition is a physical vapor deposition technique in which flux of deposition material arrives at a large oblique incidence angle (>80°) from the substrate normal (while the substrate is rotating). Fig. 2a presents a schematic of the oblique angle deposition process.

The oblique angle deposition process results in the formation of isolated nanorods by the self-shadowing effect during growth. The shadowing effect is a characteristic of oblique angle deposition and occurs when regions of relatively greater initial growth rate obstruct the flow of incident flux to other areas, causing the morphology to deviate from the smooth and regular surface that results from depositions performed at normal incidence. More information about the oblique angle deposition process can be found in Ref. [10].

The W nanorods were grown on the $LiTaO_3$ crystal using a 99.95% pure W cathode in a DC magnetron sputtering chamber with a base pressure of less than 8×10^{-7} torr. The sputtering power used was 200 W at an argon pressure of 2.3 mtorr. The crystals were mounted on a stepper motor and placed at a glancing angle ($\theta = 85°$) with respect to the sputter target, and the motor was rotated at an angular velocity of 0.5 Hz. There was no intentional heating or cooling of the

Please cite this article in press as: D.J. Gillich, et al., Nano Today (2009), doi:10.1016/j.nantod.2009.04.004

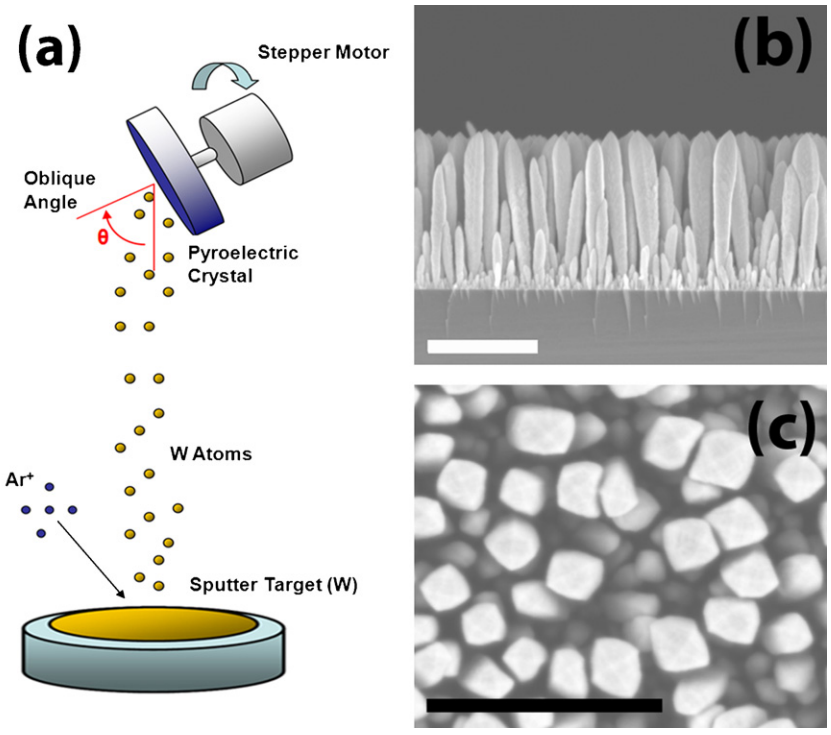

Figure 2 (a) Diagram of the oblique angle deposition technique used to grow nanorods onto the pyroelectric crystal. (b) SEM side-view picture of W nanorods on a Si substrate. (c) SEM top-view picture of W nanorods on a Si substrate. Both Fig. 1b and c have a 400 nm scale bar.

crystals during the deposition. The limited adatom mobility combined with the shadowing effects due to the extreme oblique incidence, resulted in the formation of isolated W nanorods. The nanorods were grown to be approximately ~175 nm high (as measured in separate experiments on a Si wafer) and have pyramidal apex shaped tips because of competition between the different crystal planes arising from minimization of surface free energy. Fig. 2b and c provide side-view and top-view SEM pictures of W nanorods on a Si substrate, respectively to highlight the shape and the tip-like structure of the W nanorods deposited on the crystal surface.

Similar pictures of the nanorods deposited directly on the crystal were not possible due to the roughness of the crystal surface. Fig. 3 presents SEM images of the bare crystal surface (a) and W nanorods deposited directly on the crystal surface before (b) and after (c) experimentation. Fig. 3a shows that the crystal surface may be sufficiently rough such that clusters of nanorods can be formed (see Fig. 3b) on the crystal surface high points or ''hills''. These clusters of nanorods may act locally as dominant electric field-enhancing tips which, over the course of emission, erode (as evident in Fig. 3c) at which time other groups of tips likely become dominant.

Once the crystals were mounted on the flanges and the system was under vacuum with average D_2 ambient operating pressure of ~20.2 mtorr, a thermal management system was used to control the thermal cycles of each crystal. A LabVIEW program provided input into two thermoelectric module temperature controllers (Oven Industries Model 5R7-388) which were used to control the heating and cooling of the crystals. The crystals were heated from ~28 °C to 130 °C over a period 5 min, allowed to soak at ~125 °C for a period of 5 min and then cooled to 30 °C over 6 min. Neutron emission occurred during the crystal cooling phase. X-ray emission was monitored using an Amptek XR-100T, Cadmium Telluride (CdTe) semiconductor diode X-ray detector. The signal from this detector was fed to a Canberra Multiport II multi-channel analyzer (MCA) and multi-channel scalar (MCS). The X-ray energy and time data was collected by

Table 1 Comparison of experimental data from three different types of experiments: a pyroelectric crystal with a single 70 nm radius tip, with W nanorods grown directly on the surface, and with W nanorods grown on a W substrate on the crystal surface. The data represents the weighted average and weighted standard deviation [12] of the results from three experiments.

	Single 70 nm tip	W nanorods directly on crystal face	W nanorods with a tip
X-ray energy (keV)	145 (±1)	185 (±17)	156 (±15)
X-ray yield (counts)	1.6 (±0.2) × 10^6	4.1 (±0.6) × 10^6	3.3 (±0.4) × 10^6
Net neutron counts	93 (±7)	61 (±34)	371 (±42)

Please cite this article in press as: D.J. Gillich, et al., Nano Today (2009), doi:10.1016/j.nantod.2009.04.004

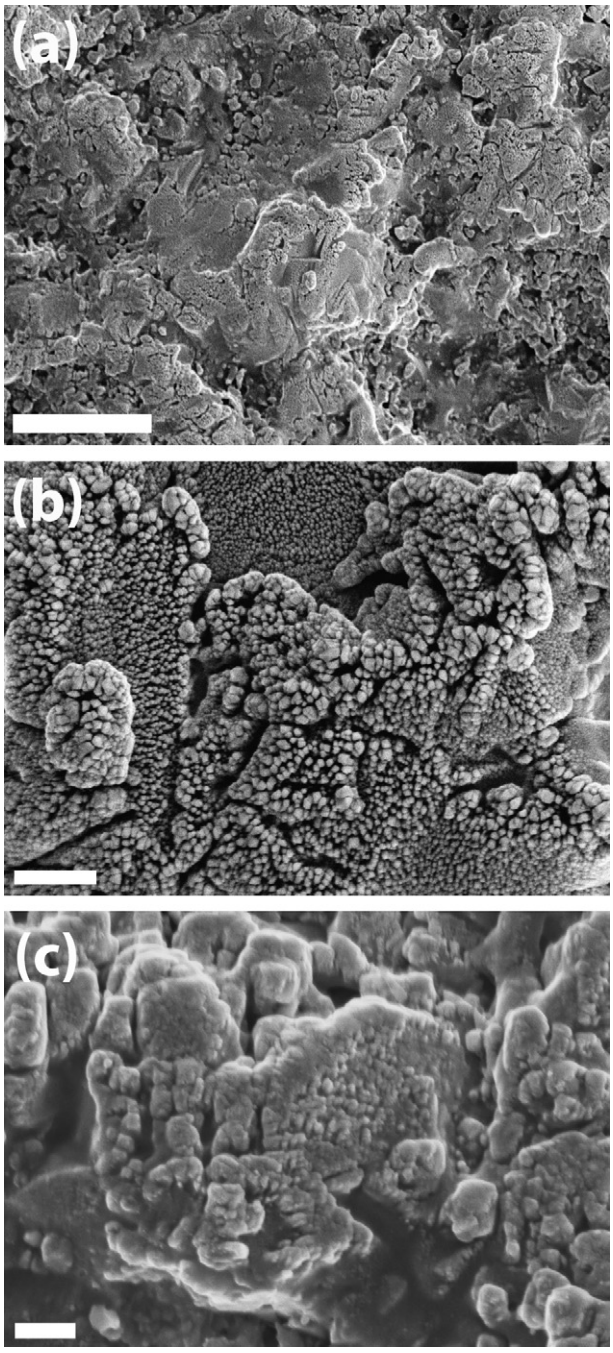

Figure 3 SEM images of (a) the crystal face with a scale bar of 4 μm to show the roughness of the crystal surface, (b) nanorods deposited directly on the crystal surface before experimentation with a 400 nm scale bar and (c) a picture of the nanorods deposited directly on the crystal surface after 20 experiments with a 400 nm scale bar.

GENIE 2000 Virtual Data Manager Software. The nanorods were examined by a scanning electron microscope (SEM, Zeiss Supra 55 FESEM at 10.0 kV) before and after the experiments were conducted.

A 5-in. diameter by 3-in. thick proton-recoil detector (Eljen 510-50 × 30-9/301) which was coupled to a Photonics photomultiplier tube (VD105K/01) detected neutrons through a 6 mm sheet of lead which was used to reduce the number of X-rays incident on the detector face. Data from the neutron detector was collected using an Acqiris AP240 PCI analyzer board and analyzed using software developed at RPI [11]. The detector pulses were analyzed using pulse fall-time discrimination curves to discriminate neutrons from gamma radiation [5].

Table 1 provides a comparison of the experimental data from the three different types of experiments. The data was collected during the 6-min cooling period from three separate experiments for each type of experimental setup. The data includes the weighted average X-ray energy and counts and net neutron counts with the weighted standard deviation [12] for the three experiments.

In Fig. 3b, the square or diamond shape of the nanorods indicates that the nanorods have distinct tips before experimentation. The nanorods pictured in Fig. 3c experienced 20 separate experiments consisting of 16 min thermal cycles (5 min heating to ~130 °C, 5 min soaking at ~125 °C, and 6 min cooling to ~30 °C, using linear heating and cooling ramps) and associated charging and discharging of the crystals. Fig. 3c shows obvious rounding of the nanorods at the tip. The rounding of the nanorod tip-like structure was probably due to tip erosion that has been reported previously in experiments using one tip [4]. The evaporation/melting of tip material can be attributed to the high current densities, arcing due to discharge and plasma conditions near the surface of the crystal. The current density for a single nanorod tip could be as high as 20 kA/cm^2 if it is assumed that the entire ion current is emitted from a single dominant nanorod tip. It is more likely that the current density that individual nanorods encounter is orders of magnitude lower because the ion current is dispersed over potentially thousands of dominant nanorod tips over the entire crystal face.

Because discharges occur at different times in a thermal cycle and averaging several experimental results over time does not give a true depiction of individual experiments, Fig. 4 provides a comparison of single experiments for each of the three types of data collected: Fig. 4a presents the X-ray end point energy over time, Fig. 4b shows the X-ray energy emission over time, and Fig. 4c is the gross neutron counts per time (data is presented in 10 s bins). The X-rays detected during the experiments are Bremsstrahlung X-rays from decelerated electrons impacting the tip crystal. These X-rays give an indication of the acceleration field that ions experience (the end-point energy) and the ion current (the X-ray yield). The background in the neutron window over a 6 min period is approximately 49 counts. Subtracting the background and accounting for the solid angle and detector efficiency, the 371 (±42) net neutron counts equates to about 7×10^3 neutrons produced over the thermal cycle.

Fig. 4b shows significant peaks in the X-ray count over time are referred to as ''plasma peaks'' by the RPI group. Plasma peaks are periods when an increase in X-ray energy and intensity and enhanced neutron production has been observed [5]. In subsequent work, a bright glow, thought to be plasma was observed at the tip during periods of enhanced neutron production [13].

Comparing the first type of experiment (tip alone) to the second type (nanorods alone), the data in Table 1 and Fig. 4 shows that while a single tip was more efficient in terms of producing neutrons, the X-ray yield and energy was higher

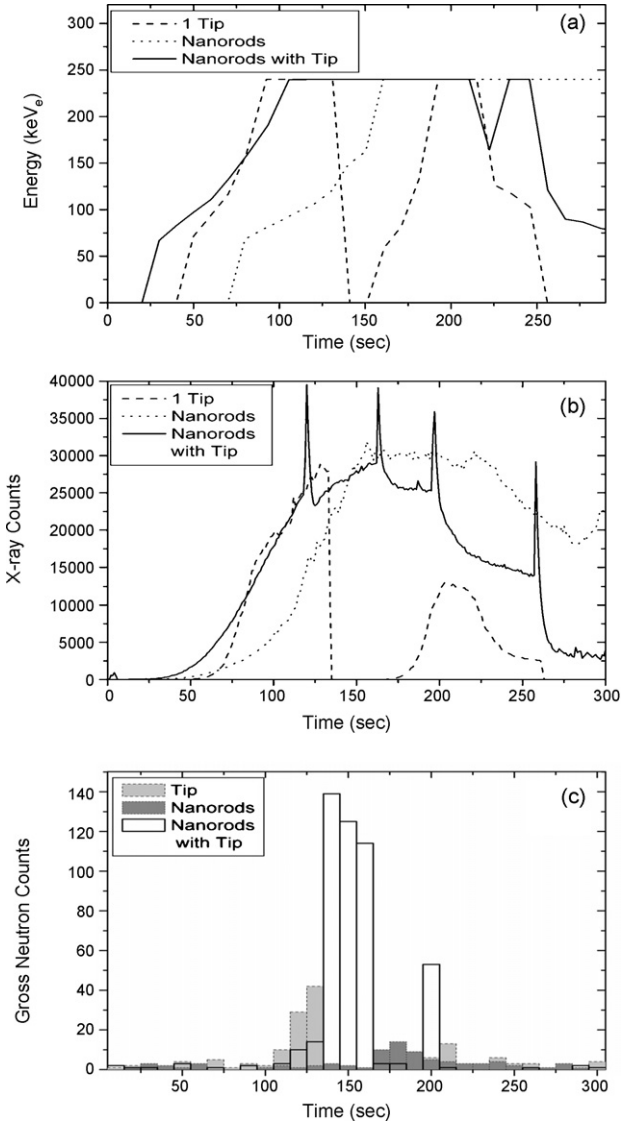

Figure 4 Results from single experiments: one 70 nm radius W tip, ~225 nm tall W nanorods directly on the crystal surface, and nanorods with tip. (a) X-ray energy over time, (b) X-ray yield over time, and (c) is gross neutrons over time (10 s bins) the background is about 10%. In (a), the straight line indicates that the detector was saturated at ~240 keV.

with the nanorods. The reason for these results may be that while the nanorods are better at ionizing the D_2 gas they do not provide a focused ion current to the target crystal and as a result fewer ions are hitting the target. It is also possible that although the ionization was intense as indicated by the X-ray yield, the ionization mostly created D_2^+ ions instead of D^+ which would result in a reduction in neutron yield. Due to strong ionization, it is believed that the nanorods produce plasma near the crystal surface such that ions near the surface quickly recombine.

The surface area increases necessarily as a result of the tungsten nanorod film deposition, but the effective emission surface area actually decreases compared with a planar surface due to the roughness of the crystal surface. The tungsten nanorod deposition does, however, increase the number of effective electric field-enhancing tips available to ionize the D_2 gas near the crystal surface. While the addition of the tungsten nanorods increased the effective number of tips, simply coating the crystal with nanorods did not significantly increase the neutron yield. This result may be due to a couple of reasons: the electric field-enhancement from the nanorod tip clusters may not be as high as a single tip and/or the ion current produced near the nanorod tip clusters may not be focused onto the target.

Fig. 5 provides evidence of the difference in ion current for a single tip versus nanorods from one crystal to the other. A Starlight Express, SXVF-M7, 16 bit black and white camera was used to take pictures of the system during a cooling cycle. Fig. 5a is a picture of a discharge from a tip which shows focused plasma to the target (and to ground). Fig. 5b is a picture of a discharge from nanorods deposited on the surface of the crystal which shows that the plasma discharges from the entire surface of the crystal. Because the vacuum chamber used to achieve the results in this paper cannot be fitted with a viewport, these pictures were taken in a different vacuum system. In the pictures the crystals were only ~2.1 cm apart from each other. Therefore, the reduction in a focused ion current effect is amplified in crystals that are ~7 cm apart as was the case in the experiments described in this paper.

The experiment with the combination of nanorods and tip yielded higher neutron counts but lower X-ray energy and yield compared to nanorods alone. The enhanced neu-

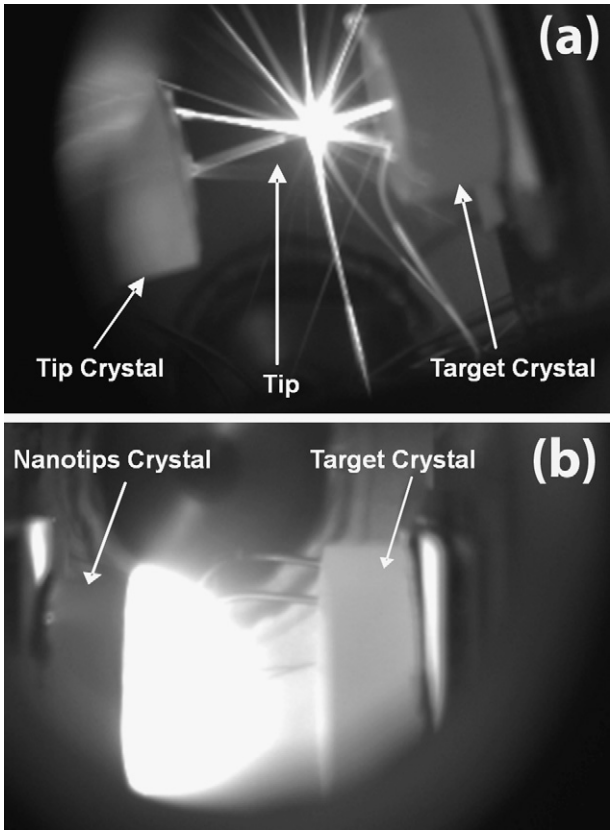

Figure 5 Pictures of discharge from a single 70 nm radius W tip (a) and from nanorods directly on the surface of the crystal (b). The crystals in these pictures are 2.1 cm apart.

Please cite this article in press as: D.J. Gillich, et al., Nano Today (2009), doi:10.1016/j.nantod.2009.04.004

tron production may be due to two ionization mechanisms: a primary ionization effect due to the nanorods at the crystal surface and a secondary ionization effect at the tip. A reduced X-ray yield may be explained by more electrons migrating to the relatively higher electric field near the tip which would decrease the number of electrons impacting the crystal face ultimately making less Bremsstrahlung X-rays. Electrons may be decelerated due to the same high electric field near the tip which would explain a reduction in the X-ray energy as well.

Because the single tip erodes significantly over time, it may be beneficial to create a system without a tip. Patterning the nanorods onto the crystal surface may help achieve a more focused current to ensure more ions impact the target while omitting the necessity of a tip. A method similar to that presented in Ref. [14] which includes the use of a focused laser beam to pattern CuO nanorods on a substrate may be necessary. Patterning may also help to more evenly distribute current density which would enhance the structural integrity of the nanorod tips.

In conclusion, W nanorods with a tip have been used to enhance D–D fusion using pyroelectric crystals. While the neutron yield was not as high as previously achieved [1–3], the results do show that nanorods used in conjunction with a tip can increase neutron production compared to a tip or nanorods alone. Patterning nanorods on the crystal surface may prolong the lifetime of the nanorod tip structure thereby achieving meaningful progress toward a neutron generator with long life.

Acknowledgment

This work was supported by DHS cooperative agreement number 2007-DN-077-ER0003.

References

[1] B. Naranjo, J. Gimzewski, S. Putterman, Nature 434 (2005) 1115.
[2] J. Geuther, Y. Danon, F. Saglime, Phys. Rev. Lett. 96 (2006) 054803.
[3] V. Tang, et al., Rev. Sci. Instrum. 78 (2007) 123504.
[4] D. Gillich, A. Kovanen, B. Herman, T. Fullem, Y. Danon, Nucl. Inst. & Methods A 602 (2) (2009) 306.
[5] J.A. Geuther, Radiation generation with pyroelectric crystals, Ph.D. Thesis, Rensselaer Polytechnic Institute, Troy, NY, 2007.
[6] S.B. Lang, Phys. Today 58 (August) (2005) 31.
[7] J.D. Brownridge, S.M. Shafroth, in: W.T. Arkin (Ed.), Trends in Lasers and Electro-Optics Research, Nova Science Publishers Inc., London, 2006, pp. 59–95.
[8] D. Gillich, Y. Danon, J.A. Geuther, B. Marus, B. McDermott, ANS Trans. 97 (2007) 927–928.
[9] J.P. Singh, T. Karabacak, T.-M. Lu, G.-C. Wang, N. Koratkar, Appl. Phys. Lett. 85 (2004) 3226.
[10] K. Robbie, M.J. Brett, J. Vac. Sci. Technol. A 15 (1997) 1460.
[11] F.J. Saglime, Y. Danon, R. Block, Digital data acquisition system for time of flight neutron beam measurements, in: ANS 14th Bien. Topical Meeting of Rad. Protect. & Shield. Div. [CD Rom], Carlsbad, New Mexico, USA, 2006, pp. 527–529.
[12] F Yu, Yaborov, INDC(CCP)-343, 1991.
[13] D. Gillich, Y. Danon, A. Kovanen, B. Herman, W. Labarre, ANS Trans. 98 (2008) 393–394.
[14] T. Yu, et al., Nanotechnology 16 (2005) 1238.

Lieutenant Colonel Don Gillich received his B.S. in Mathematics from Florida Southern College in 1989; he also received a commission in the US Army through ROTC and entered active service. After several assignments, Don attended the Naval Postgraduate School where he received an M.S. degree in Physics. After teaching at the United States Military Academy for 3 years, Don was given the opportunity to return to academia via RPI to earn a Ph.D. in nuclear engineering. Upon graduation, Don will return to the Department of Physics at West Point.

Ranganath Teki obtained a Bachelors degree from Indian Institute of Technology, Madras, India and a Masters from Johns Hopkins University, Baltimore, U.S.A.—both in Chemical Engineering. He is currently pursuing his Ph.D. in Chemical Engineering at Rensselaer Polytechnic Institute, Troy, U.S.A. His current research focuses on growth of nanoscale structures by oblique angle deposition using sputtering and their applications in energy conversion devices.

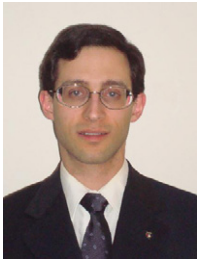

Dr. Travis Z. Fullem received the B.A. degree in physics (with honors) from Ithaca College and attended Binghamton University for graduate school where he received M.S. degrees in both physics and electrical engineering and the Ph.D. degree with dissertation research on the heat transfer properties of thermal interface materials. He is currently a Postdoctoral Research Associate in the Department of Mechanical, Aerospace and Nuclear Engineering at Rensselaer Polytechnic Institute. Prior to receiving his Ph.D., he was an intern at Knolls Atomic Power Laboratory and spent a year as a National Science Foundation GK-12 Teaching Fellow.

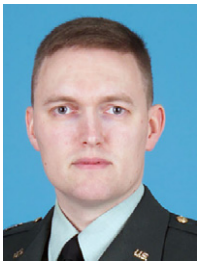

Major Andrew Kovanen graduated from the United States Military Academy at West Point in 1999 with a B.S. in Engineering Physics. Upon commissioning, he spent 8 years at various assignments as an Army Signal Corps officer. In 2007 Andrew was selected to serve as a Nuclear and Counterproliferation officer and sent to Rensselaer Polytechnic Institute (RPI) for advanced studies. He currently conducts research with the goal of developing a portable neutron generator using pyroelectric crystals. After receiving his M.S. in Nuclear Engineering, Andrew will return to West Point for a 3-year tour teaching physics and nuclear engineering.

Ezekiel Blain received his Bachelors degree in Nuclear Engineering from Rensselaer Polytechnic Institute located in Troy NY in 2008. He is currently pursuing a doctoral degree in Nuclear Engineering and Sciences from Rensselaer Polytechnic Institute. His current research focuses on non-destructive nuclear testing for assay of spent nuclear fuel using a lead slowing down spectrometer.

Professor Douglas B. Chrisey is a Professor of Materials Science at Rensselaer Polytechnic Institute. He received his Ph.D. in Physics from the University of Virginia in 1987 and then joined the US Naval Research Laboratory. He spent the next 17 years there and his research interests include the novel laser fabrication of thin films and coatings of advanced electronic, sensor, biomaterial, and energy storage. These materials were used in device configurations for testing and typically have an improved figure-of-merit. He is considered one of the pioneers in the field of Pulsed Laser Deposition and was the lead inventor of MAPLE processing technique. His research has resulted in more than 400 citable publications and over 5000 citations and he has edited or co-edited 15 books and has 18 patents. He also serves as the Chief Technology Officer for Nano Solutions and is President of Omni-Metrics.

Dr. Toh-Ming Lu, the Ray Palmer Baker Distinguished Professor of Physics, was the former Chairman of the Physics Department at Rensselaer Polytechnic Institute (1992—1997). He was the Director of the Center for Advanced Interconnect Science and Technology (1999—2005), a multi-university center involving 13 universities, 25 faculty, and 40 graduate students. His research interest is in materials physics. His honors include: Fellow of American Physical Society (1994); Fellow of American Vacuum Society (1995); Fellow of the American Association for the Advancement of Science (2007); Fellow of the Materials Research Society (2008); Materials Research Society Medal Award (2004); and Semiconductor Research Corporation Faculty Leadership Award (2005).

Dr. Yaron Danon received his Ph.D. from RPI in 1993; he then worked at the Nuclear Research Center Negev until 2000 when he returned to RPI as faculty. Dr. Danon is an Associate Professor in the Department of Mechanical Aerospace and Nuclear Engineering and the Director of the Gaerttner LINAC Laboratory. His research interests include: nuclear data, novel X-ray and neutron sources, novel radiation detectors, nondestructive testing, medical isotope production and radiation transport. Dr. Danon published over 100 scientific papers and currently advises 10 Ph.D. students and 2 M.S. students.

Please cite this article in press as: D.J. Gillich, et al., Nano Today (2009), doi:10.1016/j.nantod.2009.04.004